THE JOURNAL OF BIOLOGICAL CHEMISTRY
Vol. 278, No. 50, Issue of December 12, pp. 50212–50216, 2003

Printed in U.S.A.

Single-walled Carbon Nanotubes Are a New Class of Ion Channel Blockers*

Received for publication, September 15, 2003, and in revised form, September 30, 2003
Published, JBC Papers in Press, September 30, 2003, DOI 10.1074/jbc.M310216200

Ki Ho Park‡, Manish Chhowalla§¶, Zafar Iqbal‖, and Federico Sesti‡**

From the ‡Department of Physiology and Biophysics, University of Medicine and Dentistry of New Jersey, Robert Wood Johnson Medical School, Piscataway, New Jersey 08854, the §Department of Ceramic and Materials Engineering, Rutgers University, Piscataway, New Jersey 08854, and the ‖Department of Chemistry and Environmental Science, New Jersey Institute of Technology University Heights, Newark, New Jersey 07102

Here we identify a novel class of biological membrane ion channel blockers called single-walled carbon nanotubes (SWNTs). SWNTs with diameter distributions peaked at ~0.9 and 1.3 nm, C_{60} fullerenes, multi wall nanotubes (MWNTs), and hyperfullerenes (nano-"onions") were synthesized by several techniques and applied to diverse channel types heterologously expressed in mammalian cells. External as-fabricated and purified SWNTs blocked K^+ channel subunits in a dose-dependent manner. Blockage was dependent on the shape and dimensions of the nanoparticles used and did not require any electrochemical interaction. SWNTs were more effective than the spherical fullerenes and, for both, diameter was the determining factor. These findings postulate new uses for SWNTs in biological applications and provide unexpected insights into the current view of mechanisms governing the interaction of ion channels with blocking molecules.

Because of the physiological role they play, ion channels exhibit unique structures, including the pore that provides the physical pathway for ion movements across the plasma membrane and several charged domains that attract and/or repel ions (1). These characteristics make ion channels easy targets for external agents such as natural toxins and synthetic drugs that react with them by establishing electrochemical interactions. Thus, blocking agents have been used not only as the basic components for commercial pesticides and potential therapeutic drugs but also to infer functional information (1).

The identification of new classes of molecules to target ion-channels is of significant interest in biological research, and, therefore, we sought to explore the possibility of using novel materials such as selected single-walled carbon nanotubes (SWNTs),[1] as ion channel blockers. In recent years there have been several attempts to use nanotubes for biological purposes because of their unique mechanical, chemical, and electrical properties (2). For example, nanotubes have been successfully used for the helical crystallization of proteins (3) and the growth of embryonic rat brain neurons (4) and as potential biosensors and bioreactors (5, 6). Here we show that SWNTs of certain diameters can efficiently block K^+ channels.

MATERIALS AND METHODS

Nanotubes and Fullerene Synthesis—SWNTs, with a diameter distribution peaked in the 0.8–0.9 nm range, were grown by chemical vapor deposition (CVD) in a horizontal tube reactor using a three-stage process. In the first stage, the catalyst/support system was obtained via wet mixing followed by combustive calcination. Magnesium nitrate hexahydrate, cobalt nitrate hexahydrate, ammonium heptamolybdate tetrahydrate, and citric acid (the latter to induce combustion) were mixed with enough distilled water to give a clear solution, which was heated to 550 °C for 5–10 min in air. The resulting powder of general composition $MgO_{(1-x-y)}Co_xMo_y$ (where nanoscale Co-Mo is the catalyst in a typical molybdenum/cobalt atomic ratio of 1:4, and MgO is the catalyst support) was taken out, ground to a fine consistency, and placed in a quartz boat in the CVD reactor. The deposition reaction zone was pumped down to 10^{-3} torr, back-filled with pure hydrogen to 1 atm, and the temperature was raised to 500 °C for 30 min. The temperature was then raised to 700 °C, and pure CO was introduced at 1 atm with a flow rate of 100 standard cubic centimeters per minute. The SWNT growth was carried out for 20 min. For purification, the as-prepared SWNTs, together with the catalyst and support, were immersed in 6 M hydrochloric acid, shaken for a few minutes, centrifuged, and decanted. The roughly purified SWNTs were dispersed again in 6 M hydrochloric acid, sonicated for 5–10 min, centrifuged, and decanted. This process was repeated twice. The purified SWNTs were then washed 2–3 times with de-ionized water, filtered, and dried. X-ray diffraction and x-ray photoelectron spectroscopy of the SWNT powder showed the absence of MgO and catalyst particles. The purified SWNTs (consisting only of SWNTs as determined by micro-Raman scattering spectroscopy and x-ray diffraction) were used after dispersion to a uniform and stable suspension by ultrasonic agitation for 15 min in a basic aqueous solution (pH near 10) containing 1 volume percentage of Triton X-100 surfactant. The purification of the Tubes@Rice SWNTs was carried out with 45 h of reflux in 2–3 M nitric acid to remove amorphous carbon and graphitic onions. Following reflux, the suspension was centrifuged, and the supernatant fluid was decanted. The SWNT sediment was washed, resuspended, centrifuged, and again decanted. This process was repeated 3–4 times. The purified SWNTs were dispersed in a pH 10 aqueous solution containing 0.5 volume percentage Triton X-100 by ultrasonic agitation for ~1 h. Stock solutions were prepared by rinsing the nanomaterials in water several times (until they formed clusters indicating removal of Triton) and resuspended in CHAPS. To confirm that this treatment was sufficient to remove Triton, nanotubes in which Triton was removed via annealing in a nitrogen atmosphere at 300 °C for 2 h were tested on HERG channels. The absence of the Triton subsequent to annealing was confirmed by Fourier transform infrared spectroscopy. Annealed nanotubes retained their blocking efficiency (data not shown), indicating that blocking can be attributed to nanotubes alone and not to the Triton.

Electrophysiology—CHO cells were transiently transfected with

* This work was supported in part by National Institutes of Health Grant R01GM68581-01 (to F. S.).The costs of publication of this article were defrayed in part by the payment of page charges. This article must therefore be hereby marked "*advertisement*" in accordance with 18 U.S.C. Section 1734 solely to indicate this fact.

¶ To whom correspondence may be addressed: Rutgers University, Ceramic and Materials Engineering, 607 Taylor Rd., Piscataway, NJ 08854. Tel.: 732-445-5619; Fax: 732-445-3258; E-mail: manish1@rci.rutgers.edu.

** To whom correspondence may be addressed: University of Medicine and Dentistry of New Jersey, Robert Wood Johnson Medical School, Dept. of Physiology and Biophysics, 675 Hoes Lane, Piscataway, NJ 08854. Tel.: 732-235-4032; Fax: 732-235-5038; E-mail: SESTIFE@UMDNJ.EDU.

[1] The abbreviations used are: SWNT, single-walled carbon nanotube; CVD, chemical vapor deposition; CHAPS, 3-[(3-cholamidopropyl)dimethylammonio]-1-propanesulfonic acid; HERG, human ether-a-go-go-related gene; CHO, Chinese hamster ovary; MWNT, multi-wall nanotube; TEM, transmission electron microscope.

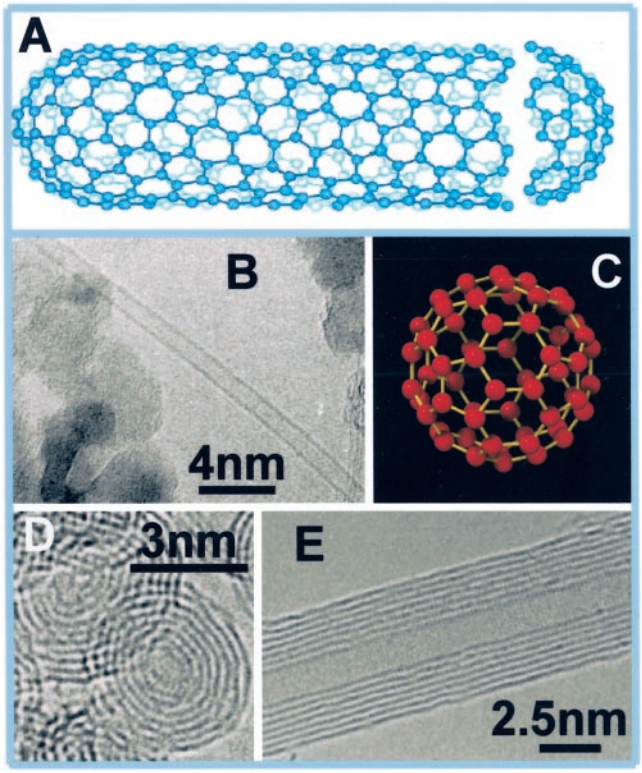

FIG. 1. **Types of nanostructures investigated in this study.** *A*, schematic of a (10,5) chiral SWNT with a bisected fullerene as the cap. *B*, transmission electron microscope (TEM) image of an isolated SWNT grown by CVD (17). In addition to the CVD-grown SWNTs, laser oven-synthesized SWNTs from Tubes@Rice (18) were also investigated. The diameters of the two types of SWNTs were determined by Raman scattering. The CVD and Tubes@Rice SWNTs were found to have peaked diameter distributions of 0.9 nm and 1.3 nm, respectively. The average length of both types of SWNTs was determined to be ~1 μm. *C*, schematic of the C_{60} fullerene molecule with a diameter of 0.72 nm. The 99.9% pure fullerene powder obtained from Aldrich was dispersed in CHAPS. *D*, TEM image of hyperfullerenes. The so-called onions were fabricated via transformation of the nanodiamond in a TEM (19). The diameters of the larger nanostructures were determined directly through TEM images. The average diameter of the onions was determined to be 3–5 nm. *E*, TEM image of a MWNTs synthesized using a catalyst-free, carbon-arc technique (20). The average diameter and lengths of the MWNTs was found to be 10–15 nm and 1 μm, respectively.

cDNA ligated into pCI-neo using Superfect kit (Qiagen) and studied after 24–36 h. Data were recorded with an Axopatch 200B (Axon), a PC (Dell), and Clampex software (Axon), filtered at 1 kHz, and sampled at 2.5 kHz. Bath solution was 4 mM KCl, 100 mM NaCl, 10 mM Hepes (pH = 7.5 with NaOH), 1.8 mM $CaCl_2$, and 1 mM $MgCl_2$. Pipette solution was 100 mM KCl, 10 mM Hepes (pH = 7.5 with KOH), 1 mM $MgCl_2$, 1 mM $CaCl_2$, and 10 mM EGTA (pH = 7.5 with KOH). Prior to electrophysiological measurements, test solutions were prepared by diluting stocks in bath solution, and control solutions were supplemented with equal levels of CHAPS. Holding voltage was −80 mV for all experiments with an interpulse interval of 1 s if not otherwise stated.

RESULTS AND DISCUSSION

Carbon atoms can be arranged into diverse geometries forming a number of stable nanostructures. For example, a graphene sheet can be seamlessly folded to form a long, single-wall, carbon nanotube with a diameter of ~1 nm (Fig. 1, *A* and *B*). Bare carbon atoms can also be organized into spherical structures such as fullerenes. The most stable and readily available fullerene (Fig. 1*C*) is the C_{60} molecule, having an average diameter of 0.72 nm. In addition to these single layer structures, large nanotube and fullerenes can also be synthesized by superimposing concentric spherical or tubular layers to form onion-like clusters (Fig. 1*D*) or multi-wall nanotubes (MWNT) (Fig. 1*E*). The range of diameters of the onions and MWNTs used in this study were 3–5 and 10–15 nm, respectively. To assay whether nanotubes, C_{60} fullerene, and fullerene-like onions can interact with ion-channels, we conducted electrophysiological experiments on different pore-forming channel subunits heterologously expressed in mammalian (CHO) cells. Surprisingly, as-fabricated and purified SWNTs had a significant effect on channels formed by *Caenorhabditis elegans* EXP-2, KVS-1, human KCNQ1 and Kv4.2 (not shown) as well as HERG potassium channels but not on endogenous CHO cell ClC-3 channels (Fig. 2, *A–E*) (5, 7–11). Qualitatively, these molecules acted to inhibit each current to a different extent, with KCNQ1 and HERG being the more susceptible proteins. Here, we use HERG as a representative example. Effects on EXP-2, Kv4.2, KVS-1, and KCNQ1 were significant but not conceptually different from those on HERG and are not covered in detail. Fig. 2*E* shows whole-cell HERG currents recorded in the absence and the presence of the SWNTs in the test solutions. SWNT inhibition was reversible, suggesting that the interaction takes place within extra-cellular domains of the channel. Calculated dose-response relationships for SWNTs with an average diameter of 1.3 nm fitted well to the Hill equation with $K_i = 0.023 \pm 0.003$ mg/ml and a Hill coefficient $n = 1.0 \pm 0.1$, suggesting that the blockade is not cooperative (Fig. 2*F*).

HERG channels open when depolarized to positive voltages; they are described as inwardly rectifying, however, because net ion movement through these channels is inward with symmetrical K^+. This conduction mechanism is the consequence of two singular gating characteristics, rapid inactivation and slow deactivation (12, 13), as shown by the sequence shown in Equation 1,

$$\mathbf{C} \rightleftharpoons \mathbf{O} \rightleftharpoons \mathbf{I} \qquad \text{(Eq. 1)}$$

where **C**, **O** and **I** represent the closed, open, and inactivated state respectively. Rapid inactivation means that, when the channel is opened by depolarization, it enters a non-conducting (inactivated) state passing very little current. In contrast, when the membrane potential is returned to its resting value (repolarization), the channel probably retraces its conformational steps and passes through the open state on the way back to the closed configuration. The return to the closed state, or deactivation, is slow and, therefore, the channel spends a significant time in the conducting open state. SWNTs exerted several effects on HERG gating (Fig. 3, *A–F*). They lowered the half-maximal threshold for activation (Fig. 3*A*) and speeded deactivation at any voltage (~2-fold; Fig. 3, *B* and *C*). These gating modifications, however, can account only marginally for the instantaneous decrease of the tail current (Fig. 2*E*) that appears to be the principal cause of blocking. We noticed that depolarization increased current inhibition (Fig. 3*D*), which was also dependent on the duration of the depolarizing pulse (Fig. 3*E*). Although sustained depolarization produced larger tail currents (by moving an increasingly large number of channels into the inactivated state), in the presence of SWNTs this effect was significantly suppressed (Fig. 3*E*). These observations can be interpreted by assuming that either the SWNTs impair the forward transition from the open to the inactivated state ($\mathbf{O} \rightarrow \mathbf{I}$) or that, alternatively, they impair the reverse transition ($\mathbf{I} \rightarrow \mathbf{O}$) by stabilizing the inactive state. In the presence of SWNTs, the number of inactivated channels was significantly increased compared with control conditions (Fig. 3*F*), and, thus, we conclude that the blockade results from the combined effect of stabilizing the channel in the inactivated state and accelerating deactivation kinetics. Other mecha-

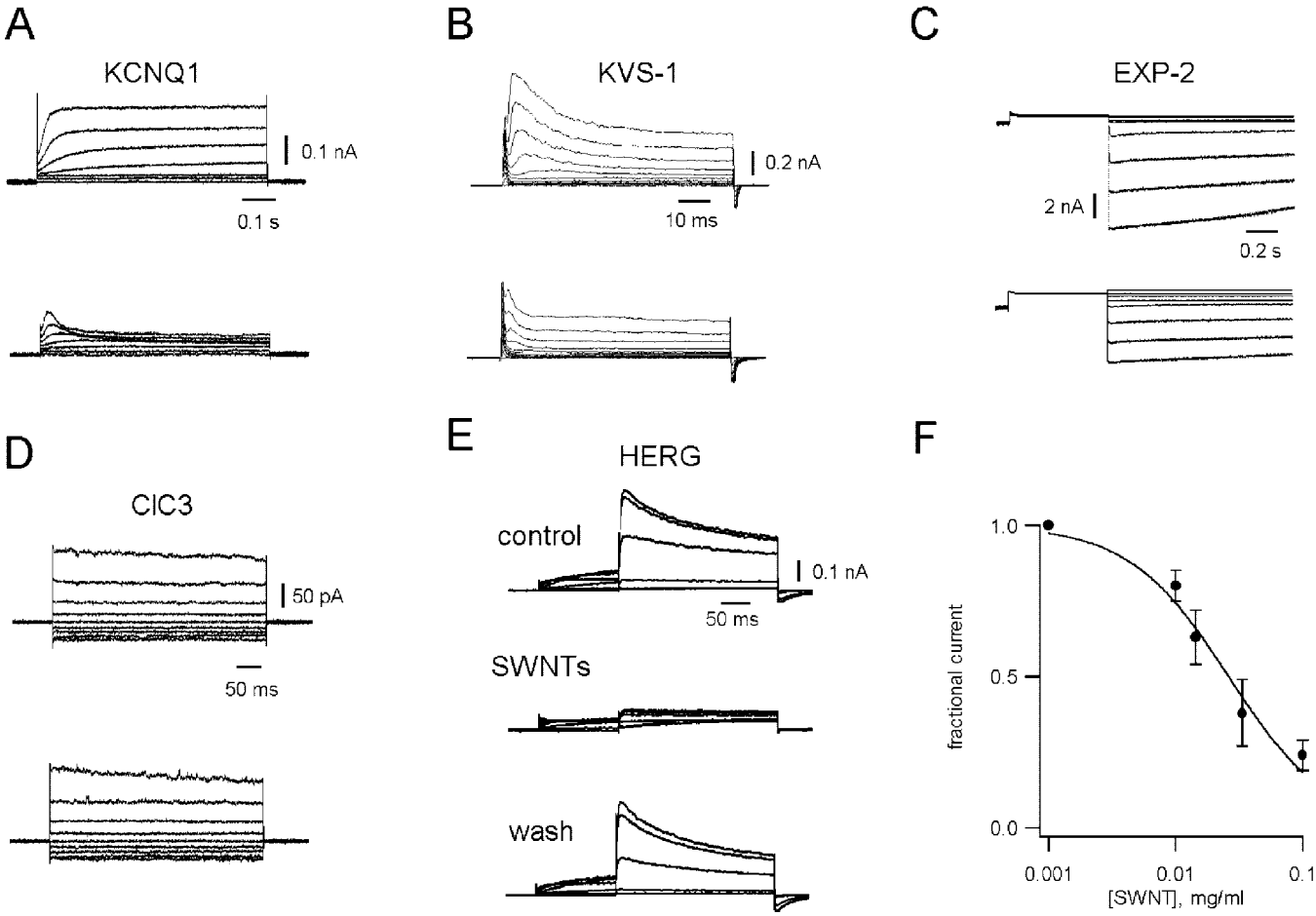

FIG. 2. **SWNTs and fullerenes interact with a variety of potassium channels in CHO cells.** In these experiments, SWNTs with diameters peaked at ~1.3 nm, and fullerenes with an average diameter of 0.72 nm were used at a 0.1 mg/ml concentration. *A*, KCNQ1 channels blocked by SWNTs. Currents were evoked by 1-s voltage steps from −80 to +40 mV in 20-mV increments. *B*, *C. elegans* KVS-1 channels are inhibited by SWNTs. Currents were elicited by 0.1 voltage steps from −80 to +120 mV in 20 mV increments. *C*, fullerenes block *C. elegans* EXP-2 currents. Channels were studied in a high K^+ (100 mM) solution to magnify tail currents that were evoked by a prepulse to 20 mV followed by test pulses from −120 to 0 mV in 20 mV increments. *D*, chloride currents endogenously expressed in CHO cells are not blocked by SWNTs. Currents were elicited essentially as described for *panel B* by using voltage steps from −80 to +80 mV. *E*, HERG tail currents in the absence or presence of SWNTs. Currents were elicited by 0.5-s preconditioning pulses from −80 to +40 mV in 20-mV increments followed by 1-s test pulse to −40 mV. *F*, current-dose relationships in the presence of the indicated amounts of SWNTs in the bath. Tail currents were measured at the end of the repolarizing pulse, and data were fit to the Hill function $K_i^n/(K_i^n + [\text{SWNT}]^n)$ with $K_i = 0.021 \pm 0.005$ mg/ml and $n = 1.2 \pm 0.2$. Data are from five cells.

nisms seem less likely; for example, a process in which the SWNTs prevent the channel to open (**C** → **O**) could be possible in principle but would challenge the observation that depolarization facilitates block (Fig. 3*D*). The fact that as-fabricated and purified SWNTs are chemically inert suggests that the geometry and not the chemical nature of the molecule must be the primary factor governing blockade. Fig. 3*G* shows the dependence of the inhibition constant K_i, assumed to be an indicator of blocking efficiency, as a function of nanotube/nanoparticle diameter for HERG, KCNQ1, and KVS-1. The extent of the block varies among channel types, but in all cases blocking is stronger with small diameters and is suppressed with large diameter nanostructures (MWNTs did not exert any block; in Fig. 3 the K_i is fixed to the astronomical 1 kg/ml value for fitting purposes). Thus, SWNTs having an average diameter of 0.9 nm blocked better than those with a diameter of 1.3 nm with $K_i(0.9)/K_i(1.3)$ ratios of 1.9, 1.5, and 1.4 for HERG, KCNQ1, and KVS-1, respectively. Block was affected not only by the dimensions but also by the shape of the molecule. In Fig. 3*H* we compare the effects of fullerenes and nanotubes at a fixed concentration (0.1 mg/ml) in the test solution. Both small diameter nanotubes (*i.e.* SWNTs) and the C_{60} fullerene blocked HERG channels and, significantly, the former were roughly 3- to 2-fold more efficient. We conclude that geometrical factors play a key role in determining a blockade whose relative intensity is probably affected by structural differences among the various channel types.

Docking simulations with the crystal structure of *KcsA* (Fig. 4*A*) provide insights into the geometrical basis of these interactions (14). In *KcsA,* a fullerene with a diameter of 0.72 nm can fit into the mouth of the selectivity filter and, like a cork in a bottle, obstruct the flow of ions (Figs. 4, *B–C*). Similarly, larger onions or MWNTs (that have diameters ≥3 nm) would be too big to fit into this or other channel crevices. The case of SWNTs is more intriguing, considering that these structures block more efficiently than fullerenes (Fig. 3*G*). SWNT synthesis and purification can result in two physically distinct and co-existing species, namely SWNTs having spherically shaped closed ends (Fig. 4*D*) and those in which one or both ends are open (Figs. 4, *E–F*). Thus, the same considerations used for fullerenes can be evoked to explain the interaction of closed end SWNTs with the selectivity filter (Fig. 4*D*). However, open-

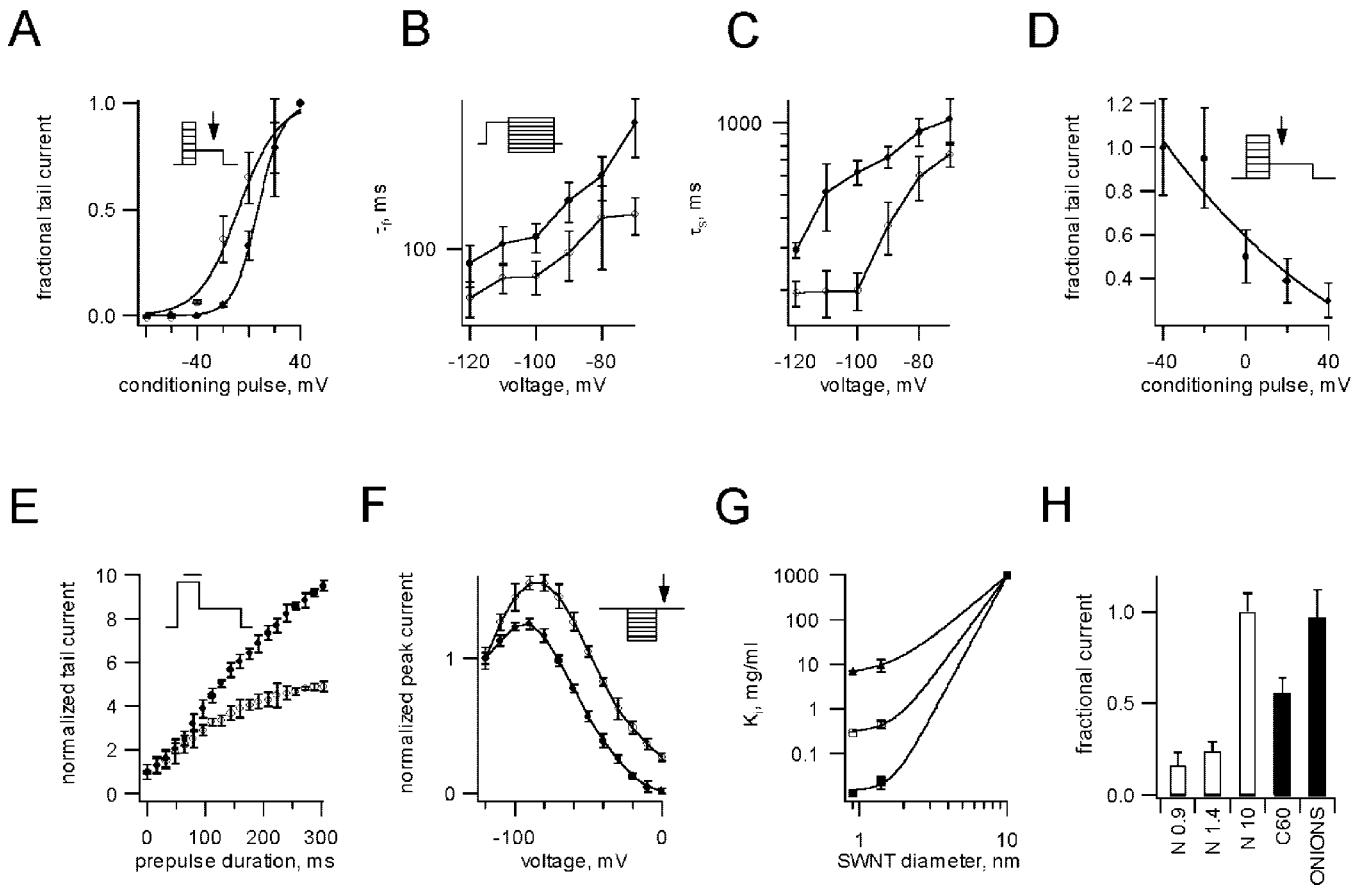

FIG. 3. **The geometrical basis of nanotube blockade.** In these experiments, *filled symbols* indicate the absence and *open symbols* the presence of 0.1 mg/ml SWNTs in the test solutions. A, steady-state activation is altered by SWNTs. Voltage protocol is in the *inset*. Lines according to the Boltzmann equation $\{1 + \mathrm{EXP}((V_{½} - V)/V_s)\}^{-1}$, where $V_{½}$ is half-maximal voltage and V_s the slope factor. $V_{½}$ was 6.9 ± 0.5 mV and −8.3 ± 2.2 mV and V_s was 9.4 ± 0.4 mV and 15.4 ± 2.0 mV in the absence and presence of SWNTs, respectively. Data are from four cells. *B* and *C*, voltage dependence of deactivation kinetics. Deactivating tail currents were evoked by the voltage protocol shown in the *inset* (0.5-s depolarizing steps to +20 mV; 1-s test pulses from −120 to 40 mV in 20-mV increments) and fitted to a double exponential function $I_o + I_f e^{-t/\tau_f} + I_s + I_s e^{-t/\tau_s}$. Data are from groups of five cells. *D* and *E*, dependence of block on the magnitude and duration of depolarization. In *panel D*, steady-state fractional tail current at −40 mV was evaluated as a function of the indicated depolarizing pulses. Depolarization increases inhibition, suggesting that opening of the channel is a prerequisite for block. Under the same conditions as in *panel D*, tail currents were evaluated in *panel E* as a function of the duration of the depolarizing step (in the *inset* in *panel D* the *bar* indicates a 20-mV variable prepulse in 16-ms increments followed by a 1-s repolarizing step to −40 mV). Data were normalized to the amplitude of the control current at time = 0. Data are from four cells. *F*, steady-state inactivation was evaluated by using a voltage protocol in which channel inactivation comes to equilibrium at various voltages during a prepulse so brief that little deactivation can occur; then, the fraction of channels in the inactive state is assessed by stepping the voltage to a test potential (*inset* depicts a 1-s depolarizing step to +20 mV, 30-ms repolarizing steps from −120 to 0 mV in 10-mV increments followed by a 1-s depolarizing step to + 20 mV). For comparison, data were normalized. Data are from groups of four cells. *G*, SWNTs block various K^+ selective pores differently. Inhibition constants were obtained by fitting dose-response curves to the Hill function (see Fig. 2*F*) and fitted to the function $a + bx^c$, with c varying from 7 to 3 in the cases considered. Nanotubes having the smallest diameter (0.9 nm) exerted maximum block on all of the three different channel types. Data are from groups of 3–5 cells. *H*, dependence of block on the shape and diameter of nanostructures. HERG channels were exposed to test solutions containing nanotubes (*N*) or fullerenes having the indicated average diameters. With both basic shapes, large diameter nanoparticles did not block the channels. In all cases, $p < 0.05$. Data are from groups of 3–5 cells.

ended SWNTs might be the most efficient type because the rim can be chemically reactive. Fig. 4, *E–F* shows open-ended SWNTs with different diameters sitting and stably anchoring on the top of the selectivity filter after having established weak electrical and/or chemical bonds. It is a common view that the three-dimensional structure of the pore and the selectivity filter is conserved among K^+ channels because of their universal TVGYG signature (15), a notion corroborated by the recent crystallization of a bacterial, voltage-gated K^+ channel (16). It is therefore not surprising that phylogenetically distant K^+ channels all appear susceptible to nanotubes, whereas chloride channels are not. Local structural differences must also exist, however, to account for the diverse extent of blocks exhibited by different channel types.

SWNTs constitute a new class of universal K^+ channel inhibitors exploiting rather elementary principles of blocking. The mechanism appears to be governed by geometrical factors and lacks any other physical/chemical component that is usually required by conventional agents. Tetraethylammonium (TEA) ions, for instance, are driven into and clog K^+ pores by their free positive charge. Short chain scorpion toxins accomplish docking by establishing electrochemical bonds with specific residues of the target protein (1). In contrast, SWNTs do not resort to any of those mechanisms but instead hamper channel function probably by fitting into the pore and thus either hindering ion movement or alternatively preventing further conformational steps. In virtue of their electrochemical neutrality, nanotubes can provide precise information about ion channel structures. For instance, our data suggest that the pore vestibules of different K^+ channel subunits such as HERG, KCNQ1, and KVS have variable dimensions, with HERG being the larger and KVS the narrower. SWNTs are

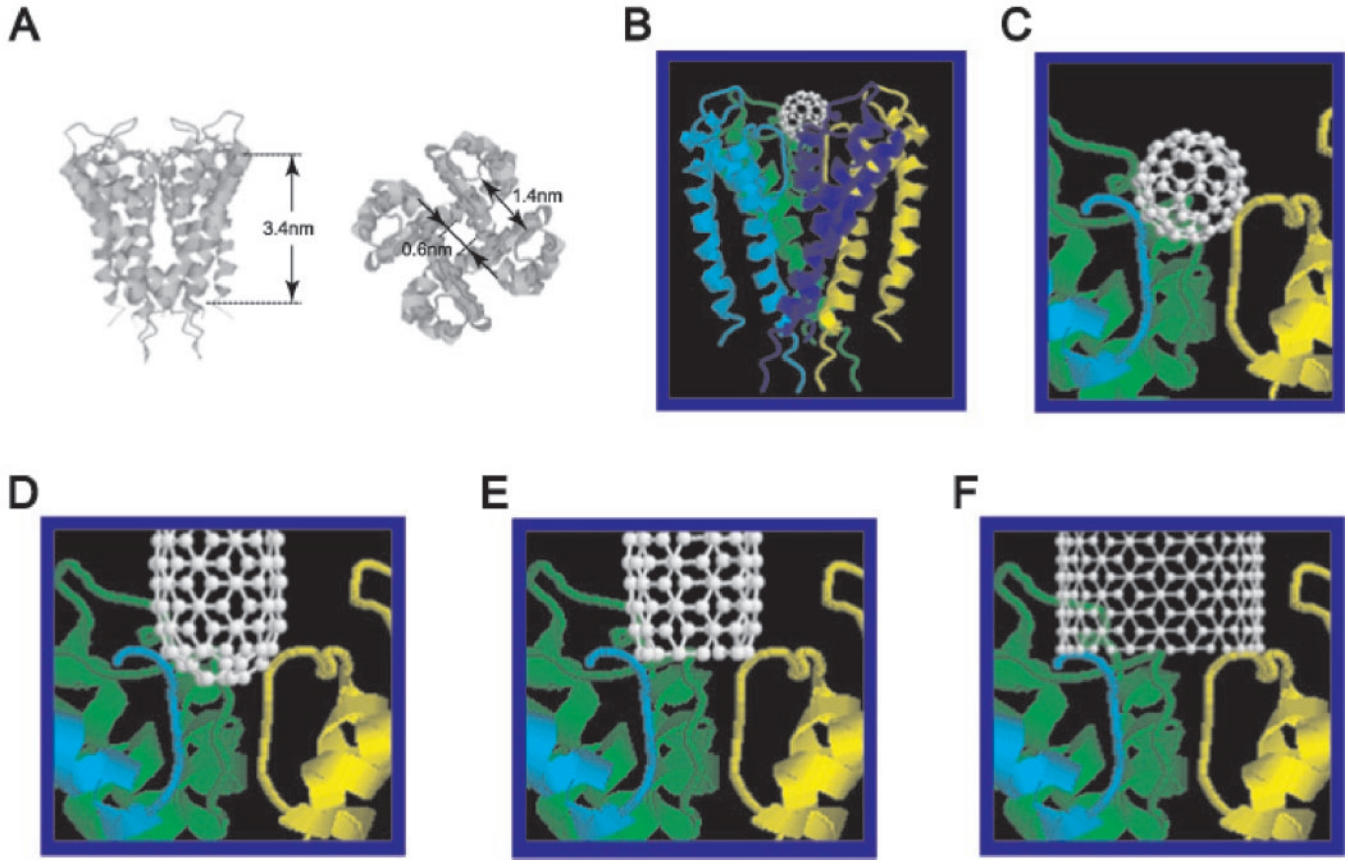

FIG. 4. **Nanotubes block K^+ channels through a pore occlusion mechanism.** *A*, the crystal structure of the *KscA* K^+ channel. This and other images were constructed by RasMol and the file 1BL8 from the Protein Data Bank. *B* and *C*, docking simulation of a fullerene. A fullerene with an average diameter of 0.7 nm can fit into the entrance of the selectivity filter and act as a cork in a bottle to stop ion permeation. *D*, docking simulation of a capped SWNT showing that, because of its spherical end, it can fit into the selectivity filter like a fullerene. The figure shows a SWNT with an average diameter of 0.9 nm, similar to those used in this report. *E* and *F*, docking simulation of an open-ended SWNT. An open-ended nanotube can sit on top of the selectivity filter establishing weak bonds. Simulations of SWNTs with average diameters of 0.9 and 1.3 nm are shown in *panels E* and *F*, respectively.

singular materials with unique characteristics. Here we unveil another previously unknown novel property of these materials that represents a further step forward in the effort to utilize them for biological purposes.

Acknowledgments—We thank Dr. S. Tomita for providing the carbon onions. EXP-2 was a gift from Dr. Leon Avery. We thank Cinzia Sesti with help with the graphics.

REFERENCES

1. Hille, B. (2001) *Ionic Channels of Excitable Membranes*, 3rd Ed., Sinauer Associates, Sunderland, MA
2. Baughman, R., Zakhidov, A., and de Heer, W. (2002) *Science* **297,** 787–792
3. Balavoine, F., Schultz, P., Richard, C., Mallouh, V., Ebbesen, T., and Mioskowski, C. (1999) *Angew. Chem. Int. Ed. Engl.* **38,** 1912–1915
4. Mattson, M., Haddon, R., and Rao, A. (2000) *J. Mol. Neurosci.* **14,** 175–182
5. Davis, J., Green, M., Hill, H., Leung, Y., Sadler, P., Sloan, J., Xavier, A., and Tsang, S. (1998) *Inorg. Chim. Acta* **272,** 261–266
6. Tsang, S., Guo, Z., Chen, Y., Green, M., Hill, H., Hambley, T., and Sadler, P. (1997) *Angew. Chem. Int. Ed. Engl.* **36,** 2198–2200
7. Bianchi, L., Kwok, S. M., Driscoll, M., and Sesti, F. (2003) *J. Biol. Chem.* **278,** 12415–12424
8. Warmke, J., and Ganetzky, B. (1994) *Proc. Natl. Acad. Sci. U. S. A.* **91,** 3438–3442
9. Li, X., Shimada, K., Showalter, L., and Weinman, S. (2000) *J. Biol. Chem.* **275,** 35994–35998
10. Wang, Q., Curran, M. E., Splawski, I., Burn, T. C., Millholland, J. M., VanRaay, T J., Shen, J., Timothy, K. W., Vincent, G. M., T., de Jager, T., Schwartz, P. J., Toubin, J. A., Moss, A. J., Atkinson, D. L., Landes, G. M., Connors, T. D., and Keating, M. T. (1996) *Nat. Genet.* **12,** 17–23
11. Zhu, X., Wulf, A., Schwarz, M., Isbrandt, D., and Pongs, O. (1999) *Recept. Channels* **6,** 387–400
12. Shibasaki, T. (1987) *J. Physiol.* **387,** 227–250
13. Smith, P., Baukrowitz, T., and Yellen, G. (1996) *Nature* **379,** 833–836
14. Doyle, D., Morais Cabral, J., Pfuetzner, R., Kuo, A., Gulbis, J., Cohen, S., Chait, B., and MacKinnon, R. (1998) *Science* **280,** 69–77
15. Heginbotham, L., Abramson, T., and MacKinnon, R. (1992) *Science* **258,** 1152–1155
16. Jiang, Y., Lee, A., Chen, J., Ruta, V., Cadene, M., Chait, B., and MacKinnon, R. (2003) *Nature* **423,** 33–41
17. Lan, A., Iqbal, Z., Aitouchen, A., Libera, A., and Grebel, H. (2002) *Appl. Phys. Lett.* **81,** 433–435
18. Thess, A., Lee, R., Nikolaev, P., Dai, H., Petit, P., Robert, J., Xu, C., Lee, Y., Kim, S., Rinzler, A., Colbert, D., Scuseria, G., Tomanek, D., Fischer, J., and Smalley, R. (1996) *Science* **273,** 483–487
19. Tomita, S., Fujii, M., Hayashi, S., and Yamamoto, K. (1999) *Chem. Phys. Lett.* **305,** 225–229
20. Iijima, S. (1991) *Nature* **354,** 56–58